31st Annual International Conference of the IEEE EMBS
Minneapolis, Minnesota, USA, September 2-6, 2009

On the Possibility to Detect Lipid in Atherosclerotic Plaques Using Intravascular Photoacoustic Imaging

Bo Wang, *Student Member, IEEE*, Jimmy Su, James Amirian, Silvio H. Litovsky, Richard Smalling, and Stanislav Emelianov, *Member, IEEE*

***Abstract*—Large lipid core is common in rupture-prone atherosclerotic plaques. Detection of the location and distribution of lipid in the atherosclerotic plaques can greatly benefit the diagnosis and treatment of vulnerable plaques. Recently introduced intravascular photoacoustic (IVPA) imaging - a technique to image the optical absorption property of tissue - can be used to detect and differentiate atherosclerotic plaques. In this work, we further investigated the ability of using spectroscopic IVPA imaging to visualize the lipid in atherosclerotic plaques. IVPA imaging was performed on an ex-vivo rabbit aorta in the 1200 – 1230 nm wavelength range. In the lipid-rich plaques, the photoacoustic signal strength within this spectral range behaved similar to the optical absorption spectrum of fatty tissue. To distinguish lipid from other types of tissue, correlation analysis was used. Specifically, intraclass correlation between the IVPA signals and the absorption spectrum of lipid reconstructed from multi-wavelength IVPA images was conducted on a pixel-by-pixel basis. The resulted correlation map showed the distribution of lipid in the atherosclerotic plaques. The distribution of lipid is further confirmed by histopathological analysis of tissue. The results of our study suggest that spectroscopic IVPA imaging, together with correlation analysis, may be used to detect lipid in atherosclerotic plaques.**

***Keywords*—intravascular photoacoustic imaging, intravascular ultrasound imaging, atherosclerosis, vulnerable plaque, lipid core, interventional cardiology**

I. Introduction

Atherosclerosis is a process that leads to a group of diseases characterized by plaques building up inside the arterial wall. Atherosclerosis claims tens of thousands of lives in the U.S. each year. Moreover, the number of deaths is growing each year, and the disease is becoming more prevalent [1]. Intense research has been focused on the detection and treatment of vulnerable plaques. One of the most common types of vulnerable plaques is the rupture-prone plaque characterized by a large lipid core, thin fibrous cap and macrophage infiltration [2]. Identification of the location of the lipid content in atherosclerotic plaques can help physicians to determine the type and vulnerability of plaques.

B. Wang, J. Su and S.Y. Emelianov* are with the Department of Biomedical Engineering, University of Texas at Austin, Austin, TX 78712 USA (*corresponding author: 512-471-1733; fax: 512-471-0616; e-mail: emelian@mail.utexas.edu).

J. Amirian and R. Smalling are with the Division of Cardiology, University of Texas Health Science Center, Houston, TX 77030 USA.

S.H. Litovsky is with the Department of Pathology, University of Alabama Birmingham, Birmingham, AL 35249 USA.

Intravascular photoacoustic (IVPA) imaging can be used to image atherosclerosis with relatively high resolution (axial resolution around 40 μm, lateral resolution around 5.5 degrees) and penetration depth of several millimeters [3]. In IVPA imaging, after irradiating the arterial tissue with nanosecond duration laser pulses, photoacoustic signals generated by the thermal expansion of the arterial tissue are acquired. The depth-resolved photoacoustic signal strength is proportional to the local optical absorption coefficient of the imaged tissue and the local laser fluence. By performing IVPA imaging at multiple wavelengths, i.e. spectroscopic IVPA imaging, the local optical absorption spectra of arterial tissues can be reconstructed. Through comparison of the multi-wavelength photoacoustic signal and the known optical absorption spectra of various tissue types, the constituents of atherosclerotic plaques may be identified [4, 5]. The spectroscopic approach has also been used to detect macrophages loaded with gold nanoparticles in molecular IVPA imaging [6].

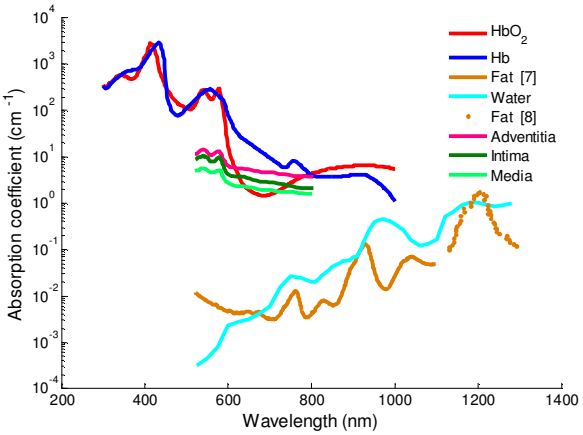

Fig. 1 Optical absorption coefficient of tissue types that may be present in vessel wall and atherosclerotic plaques [7, 8].

To detect lipid content in atherosclerotic plaques, photoacoustic imaging should be performed at the optical wavelength around 1200 nm. As shown in Fig. 1, fatty tissue has a distinct absorption spectrum different from other potential tissue types present in plaques and the vessel wall. The absorption coefficient of fatty tissue is very low below 1000 nm wavelength and becomes higher than the absorption coefficient of water in the wavelengths around 1190 – 1250 nm. The optical absorption coefficient of fatty tissue has a peak around 1210 nm wavelength, and then decreases with increased wavelength. However, the

absorption spectrum of water in this region remains relatively constant. The different absorption spectrum of fat from water can be used to identify lipid in atherosclerotic plaques.

In this study, we performed multi-wavelength IVPA imaging on a diseased rabbit aorta in the NIR wavelengths. Intraclass correlation (ICC) between multi-wavelength IVPA signals and optical absorption spectrum of the lipid was analyzed to identify the presence of lipid content within the plaques. The high correlation coefficients in the ICC result may indicate the location of lipid content. Lastly, the presence of lipid in the plaques was confirmed by histopathological analysis.

II. Materials and Methods

A. Animal Model

The New Zealand White rabbit was used as the animal model for atherosclerosis. It has been reported that fatty streaks and advanced fatty streaks can be developed in this type of rabbit through a long term low-cholesterol diet [9]. In this study, an animal was put on a low-cholesterol diet (0.2%) for 10 months. After sacrificing the rabbit, the aorta was extracted for IVPA imaging.

B. Experimental Design

The experimental setup of the imaging system is shown in Fig. 2. An OPO tunable laser that can generate laser pulses from 680 – 950 nm and 1200 – 2400 nm wavelengths was used in the experiment. The pulse duration of the laser was around 7 ns. The laser beam was coupled into an optical fiber with a core diameter of 1.5 mm. The output end of the fiber was aligned with a clinically available 40 MHz intravascular ultrasound (IVUS) imaging catheter (Boston Scientific, Inc.). The element of the IVUS transducer was faced towards the output of the optical fiber. The radio frequency (RF) signal was digitized using an A/D card operating at 200 MHz sampling rate.

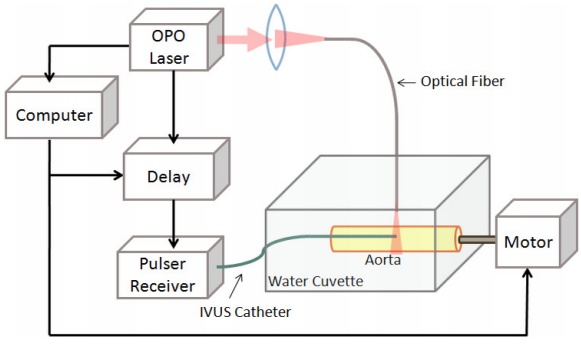

Fig. 2 Experimental setup of the IVPA and IVUS imaging system.

Once the IVUS imaging catheter was aligned with the optical fiber output, a segment of the aorta tissue measuring about 2 cm in length was immersed into saline. The aorta was irradiated with laser pulses externally, and the photoacoustic signal generated within the vessel wall was recorded using the IVUS transducer. After a user-controlled delay of 9 μs, ultrasound pulse-echo signal was generated and received by the same IVUS imaging catheter. The aorta was then rotated by a stepper motor to another angular position and IVPA/IVUS signal was recorded again. Therefore, once the motor rotated the aorta 360 degrees, co-registered IVPA and IVUS images were acquired. Each image consisted of 256 beams. After the experiment, the imaged cross-section of the aorta was marked using a surgical suture for later histopathological analysis. The histology slide was stained by Oil Red O stain for lipid and RAM11 stain for macrophages.

C. Intraclass Correlation

In order to identify the lipid content in the plaques, intraclass correlation (ICC) was applied to the multi-wavelength IVPA images [10]. ICC measures the strength of linear relationship between subjects belonging to the same class or the same subgroup or the same family. The ICC between subjects can be expressed in the following function:

$$r = \frac{2\times\sum_i (x_{i1}-\bar{x})(x_{i2}-\bar{x})}{\sum_i (x_{i1}-\bar{x})^2+\sum_i (x_{i2}-\bar{x})^2} \quad , \tag{1}$$

where x_{i1} and x_{i2} are two measurements of the ith subject, and r is the intraclass correlation output. A correlation value of more than 0.75 is considered a good agreement between two measurements [11].

In our study, ICC was used to assess the agreement between wavelength-dependent photoacoustic signal strength and the spectroscopic optical absorption property of lipid in atherosclerotic plaques. A correlation kernel size of 30 axial samples (110 μm) by 5 beams (6 degrees) was applied. To compensate the movement of the aorta tissue between scans at various wavelengths, the size of the kernel was chosen to be larger than the resolution of the imaging system. The computed correlation coefficient was assigned to the location corresponding to the middle of the kernel. The correlation analysis was performed at every position within the entire IVPA image, i.e., the kernel moved with a step size of one sample or beam. At each position, the photoacoustic signal strength from different wavelengths in the kernel was normalized and compared with the normalized absorption spectrum of lipid.

III. Results and Discussion

The IVUS image of one cross-section of the diseased rabbit aorta (Fig. 3(a)) clearly shows the morphology of the aorta. Close to the inner lumen of the aorta, hypoechoic ultrasound signals are generated from the lipid-laden plaques in the thickened intima layer; whereas the media and adventitia layer generate hyperechoic ultrasound signals. The IVPA image of the same cross-section of the aorta acquired at 1200 nm wavelength is shown in Fig. 3(b) with a dynamic range of 40 dB. From the IVPA image, it is difficult to identify the location of the optical absorber that generated the photoacoustic signal. By combining the IVPA

and IVUS images together, locations of the absorber can be identified (Fig. 3(c) and Fig. 3(d)). High intensity photoacoustic signals can be observed close to the outer boundary of the aorta because of high laser fluence in that region. Lower intensity of photoacoustic signals were generated from the middle of the aorta wall.

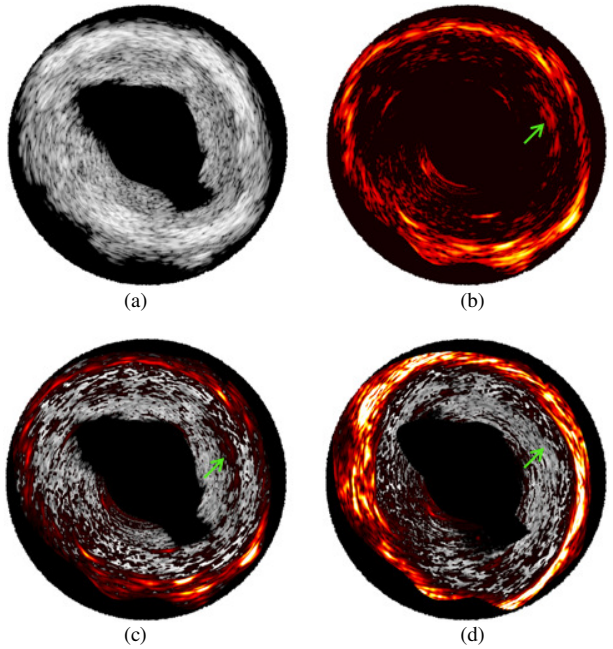

Fig. 3. IVUS cross-sectional image of the atherosclerotic rabbit aorta (a). IVPA image of the same cross-section obtained at 1200 nm wavelength (b). Combined IVPA and IVUS images at 1200 nm wavelength (c) and 730 nm wavelength (d).

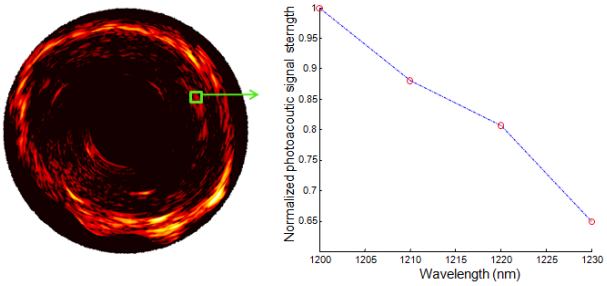

Fig. 4. The IVPA image taken at 1200 nm wavelength (left), and the normalized photoacoustic response at various wavelengths from the area denoted by green rectangle (right). The photoacoustic response from 1200 to 1230 nm with a step size of 10 nm was normalized to the signal strength at 1200 nm wavelength.

The green arrows in Fig. 3 point to a region of interest that generates photoacoustic signal at 1200 nm. However, when imaged at 730 nm, the photoacoustic signal from the same region is undetectable. As shown in Fig. 1, at the wavelength over 1000 nm, water and fatty tissue became the main absorber. Moreover, fatty tissue absorbs more than water above around 1200 nm wavelength. Thus, the photoacoustic signal indicated by the green arrow may be generated from the lipid in atherosclerotic plaques. To confirm this observation, photoacoustic strength at various wavelengths from the arrow pointed area is plotted in Fig. 4. The normalized photoacoustic signal strength shows a similar descending trend as the absorption spectrum of fat (Fig. 1), whereas the absorption spectrum of water is almost constant. Note that the absorption spectrum of the fatty tissue has a peak at 1200 nm wavelength, which is absent in the spectrum of normalized photoacoustic signal strength. The absence of the 1210 nm absorption peak may be due to the difference in absorption spectrum of fatty tissue from lipid in atherosclerotic plaques.

ICC was applied to IVPA data in 1200 - 1230 nm spectral range with a step size of 10 nm. High ICC coefficients (>0.75) were color coded and overlayed on top of the IVUS image (Fig. 5). Almost all high correlation coefficients are in the region of thickened intima layer, where lipid content is usually found in a diseased aorta. The strong photoacoustic signals in the adventitia layer (Fig. 3(b)-(d)) were not shown in the ICC result because of low correlation coefficients. The ICC result of spectroscopic IVPA data shows that the optical absorption spectrum from tissue in the outer boundary of the aorta is different from the inner lumen. Thus, the outer and inner portions of the vessel wall have different tissue types. In the wavelength ranging within 1200 – 1230 nm, the scattering from the arterial tissue is less than that in the 650 – 900 nm range. As a result, the tissue scattering plays less of a significant role in imaging using 1200 – 1230 nm spectral range. Moreover, the tissue scattering changes little within the 30 nm wavelength range where IVPA imaging was performed. Thus, even without the depth compensation for wavelength-dependent scattering in tissue, intraclass correlation can successfully differentiate tissue types.

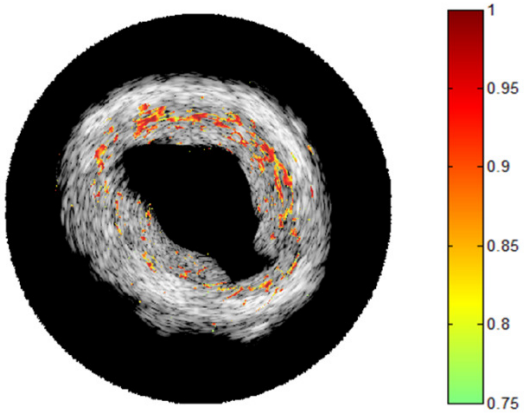

Fig. 5. Intraclass correlation coefficient with magnitude greater than 0.75 is overlaid onto the IVUS image to show the distribution of lipid content in atherosclerotic plaques.

Histopathological analysis was performed on the aorta tissue close to the imaged cross-section (Fig. 6). Histology slides show concentric lipid rich plaque occupying about 40% of the lumen. Oil Red O stain clearly demonstrates the lipid content in the inner part of the vessel wall. The location of the lipid content agrees with the ICC result in Fig. 5. Interestingly, close to the media layer, where Oil Red O

stain is relatively stronger, there is also more lipid content shown in the ICC-based image. Note that not all the lipid content in the plaques was shown in the ICC result. The reason might be that the photoacoustic signal generated from low concentration of lipids was below the detection limit of the imaging system.

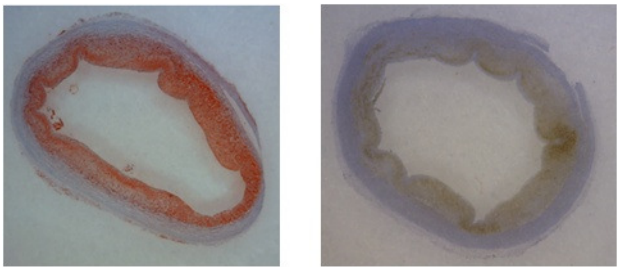

(a) (b)

Fig. 6. Oil Red O stain for lipid (a) and RAM11 stain for macrophages (b) close to the imaged cross-section of the atherosclerotic rabbit aorta.

There are several limitations because of the limited resources in this study. First, because of limited data on absorption spectrum of lipid content in atherosclerotic plaques, we used the absorption spectrum reconstructed from the photoacoustic signal in the suspected lipid region for the ICC analysis. For a more accurate analysis, the optical absorption property of lipid-rich plaques needs to be measured. Second, because of the limited wavelength range of the OPO laser source, we performed IVPA imaging in a small wavelength range (1200 – 1230 nm). Ideally, imaging should be performed in a wavelength range from around 1150 nm to 1230 nm to cover the distinct absorption spectrum of lipid from water. Third, in order to confirm the reliability of the photoacoustic spectroscopic imaging method to detect lipid in atherosclerotic plaques, future experiments will be performed using different cross-sections of the aorta on different types of atherosclerotic plaques. Note that the experiment was performed with laser light irradiated from outside of the artery. For in vivo IVPA imaging, a combined catheter needs to be developed. One option is using fiber optics to deliver light inside the artery [12].

IV. Conclusion

IVPA imaging was performed on an ex-vivo diseased aorta in the NIR wavelengths. Within the 1200 – 1230 nm wavelength range, the photoacoustic signal in the lipid-rich region of the plaque has the similar optical absorption spectrum of fatty tissue. By applying the ICC method between the multi-wavelength IVPA images and the reconstructed absorption spectrum of lipid, the location of lipid content in the plaques may be identified. The distribution of the lipid content from ICC result corresponds with the distribution of lipid in Oil Red O histological stain. Thus, spectroscopic IVPA imaging near 1200 nm wavelength has the potential to detect lipid in atherosclerotic plaques.

Acknowledgments

This work was supported in part by the National Institutes of Health under grant HL084076. The authors would like to acknowledge the technical support from Boston Scientific, Inc., and useful discussion with Mrs. Srivalleesha Mallidi related to the intraclass correlation analysis.

References

[1] W. Rosamond, K. Flegal, K. Furie, A. Go, K. Greenlund, N. Haase, S. M. Hailpern, M. Ho, V. Howard, and B. Kissela, "Heart disease and stroke statistics--2008 update: a report from the american heart association statistics committee and stroke statistics subcommittee," *Circulation,* vol. 117, p. e25, 2008.

[2] M. Naghavi, P. Libby, E. Falk, S. W. Casscells, S. Litovsky, J. Rumberger, J. J. Badimon, C. Stefanadis, P. Moreno, and G. Pasterkamp, "From Vulnerable Plaque to Vulnerable Patient: A Call for New Definitions and Risk Assessment Strategies: Part I," *Circulation,* vol. 108, p. 1664, 2003.

[3] S. Sethuraman, S. R. Aglyamov, J. H. Amirian, R. W. Smalling, and S. Y. Emelianov, "Intravascular photoacoustic imaging using an IVUS imaging catheter," *IEEE Transactions on Ultrasonics, Ferroelectrics, and Frequency Control,* vol. 54, 2007.

[4] S. Sethuraman, J. H. Amirian, S. H. Litovsky, R. W. Smalling, and S. Y. Emelianov, "Spectroscopic intravascular photoacoustic imaging to differentiate atherosclerotic plaques," *Optics Express,* vol. 16, pp. 3362-3367, 2008.

[5] T. J. Allen and P. C. Beard, "Photoacoustic characterisation of vascular tissue at NIR wavelengths," in *Photons Plus Ultrasound: Imaging and Sensing 2009*, 2009, p. 71770A.

[6] B. Wang, E. Yantsen, T. Larson, A. B. Karpiouk, J. L. Su, K. Sokolov, and S. Y. Emelianov, "Plasmonic Intravascular Photoacoustic Imaging for Detection of Macrophages in Atherosclerotic Plaques," *Nano Letters,* vol. 9, pp. 2207-2511, 2008.

[7] "Optical Absorption Spectra," http://omlc.ogi.edu/spectra/index.html.

[8] R. R. Anderson, W. Farinelli, H. Laubach, D. Manstein, A. N. Yaroslavsky, J. Gubeli 3rd, K. Jordan, G. R. Neil, M. Shinn, and W. Chandler, "Selective photothermolysis of lipid-rich tissues: a free electron laser study," *Lasers in Surgery and Medicine,* vol. 38, pp. 913-9, 2006.

[9] F. D. Kolodgie, A. S. Katocs, E. E. Largis, S. M. Wrenn, J. F. Cornhill, E. E. Herderick, S. J. Lee, and R. Virmani, "Hypercholesterolemia in the Rabbit Induced by Feeding Graded Amounts of Low-Level Cholesterol Methodological Considerations Regarding Individual Variability in Response to Dietary Cholesterol and Development of Lesion Type," *Arteriosclerosis, Thrombosis, and Vascular Biology,* vol. 16, pp. 1454-1464, 1996.

[10] S. Mallidi, J. Tam, T. Larson, A. Karpiouk, K. Sokolov, and S. Y. Emelianov, "Selective detection of cancer using spectroscopic photoacoustic imaging and bioconjugated gold nanoparticles," in *Proceedings of the 2008 IEEE Ultrasonics Symposium*, 2008, pp. 1088-1091

[11] A. Indrayan and S. B. Sarmukaddam, *Medical biostatistics*: CRC Press, 2001.

[12] B. Wang, A. B. Karpiouk, and S. Y. Emelianov, "Design of catheter for combined intravascular photoacoustic and ultrasound imaging," *Proceedings of the 2008 IEEE Ultrasonics Symposium,* pp. 1150-1153, 2008.